eXPRESS Polymer Letters Vol.12, No.2 (2018) 171–179
Available online at www.expresspolymlett.com
https://doi.org/10.3144/expresspolymlett.2018.15

Dissolution behavior of Mg/Si-doped vaterite particles in biodegradable polymer composites

P. Zhou[1], *T. Kasuga*[1,2*]

[1]Department of Frontier Materials, Nagoya Institute of Technology, Gokiso-cho, Showa-ku, 466-8555 Nagoya, Japan
[2]Division of Advanced Ceramics, Nagoya Institute of Technology, Gokiso-cho, Showa-ku, 466-8555 Nagoya, Japan

Received 21 July 2017; accepted in revised form 2 October 2017

Abstract. Tuning the ion release ability of bioactive materials is one of the key factors for bone repair and regeneration. Calcium (Ca^{2+}), magnesium (Mg^{2+}), and silicate ions were reported to enhance the activity of bone-forming cells. In this work, the dissolution behavior of magnesium- and silicate-doped calcium carbonate (vaterite), denoted as MgSiV, embedded in three kinds of biodegradable polymers in Tris buffer solutions (TBS) were examined to find an effective ion releasing system. Poly(L-lactic acid) (PLLA) and poly(D,L-lactide-*co*-glycolide) (PDLLG, lactide:glycolide = 75:25 or 50:50; denoted as PDLLG75 and PDLLG50, respectively) were chosen as the matrix polymers. The Mg^{2+} and silicate ions were released rapidly within 3 d of soaking. Continuous release of Ca^{2+} ions from the composites induced the formation of aragonite on the film surfaces in the presence of Mg^{2+} ions. The amount of ions released from the MgSiV-PLLA composite was lesser than those released from the PDLLG-based composites. The fast degradation of PDLLG50 induced a decrease in the pH of TBS. The MgSiV-PDLLG75 composite exhibited a rapid release of Mg^{2+} ions, a continuous release of Ca^{2+} ions, and a controlled release of silicate ions with no reduction in the pH of TBS. Such release phenomena are caused by the formation of pathways for ion release, originating from the water uptake ability of PDLLG75.

Keywords: *polymer composites, biodegradable polymers, calcium carbonate, ion release, biomaterials*

1. Introduction

Tissue engineering scaffolds play a decisive role in the repair and regeneration of bones [1–4]. These scaffolds provide a supporting matrix and an essential environment for cells to attach, spread, proliferate, differentiate, and mineralize. Scaffolds consisting of biodegradable polymers and bioactive materials have attracted great research attention because they can combine the tailored degradability of polymers with the osteoconductivity of bioactive materials [2, 3]. Bioactive materials, such as Bioglass® 45S5, combined with lactic acid-based polymers, showed impressive bone-forming ability [5, 6].

The ions released from 45S5 have been reported to stimulate the attachment, proliferation, differentiation, and mineralization of osteoblastic cells *in vitro* and angiogenesis both *in vitro* and *in vivo* [7–9]. The calcium (Ca^{2+}) and silicate ions released from 45S5 can stimulate osteoblast cell division and the production of growth factors and extracellular matrix proteins [9–11]. Ca^{2+} ions are necessary for bone remodeling since they directly activate intercellular mechanisms by affecting the calcium-sensing receptors in osteoblastic cells [12]. In aqueous solutions, silicate ions are associated with the formation and calcification of bone tissue [13, 14]. Magnesium (Mg^{2+}) ions have been reported to stimulate cellular activity, especially the adhesion of osteoblasts [15, 16]. These stimulatory effects on cellular activities play important roles in bone regeneration.

From these reports, it can be inferred that materials capable of releasing Mg^{2+}, Ca^{2+}, and silicate ions

*Corresponding author, e-mail: kasuga.toshihiro@nitech.ac.jp

might be beneficial as new biomaterials. In our previous work, siloxane-containing calcium carbonate (vaterite) doped with magnesium (MgSiV) was developed [17, 18]. MgSiV particles had distorted spherical shapes with a diameter of ~1.3 μm and a thickness of ~0.6 μm; they were capable of releasing Ca^{2+}, Mg^{2+}, and silicate ions in aqueous solutions. The ions released from MgSiV are expected to promote cell adhesion, proliferation, and differentiation. The ion releasing behavior of MgSiV in aqueous solutions has been reported in our earlier work [17]; it was observed that the ions were released in a short period of time. The rapid release might cause pH instability and have a significant effect on homeostasis. We propose that MgSiV can be used as a filler in polymeric composites. The ion releasing behavior of MgSiV-containing composites has not been examined so far to the best of our knowledge.

In this work, lactic acid-based polymers, such as poly(L-lactic acid) (PLLA) and poly(D,L-lactide-*co*-glycolide) (PDLLG), were used as the matrix polymers to prepare the composites with MgSiV particles as the fillers. PLLA and PDLLG belong to the family of linear aliphatic polyesters, which are often used to prepare bioactive composites. The extra methyl group in the PLLA repeating unit reduces its molecular affinity to water and leads to a slow degradation [30]. PDLLG with its higher fraction of glycolide units is likely to hydrate and swell faster than PLLA and also to degrade faster [19–22]. This work focuses on the Mg^{2+}, Ca^{2+}, and silicate ions release from MgSiV-PLLA and MgSiV-PDLLG composites in Tris buffer solutions (TBS). Changes in the surface morphologies of the composites and the pH values of the solutions are also discussed.

2. Experimental section

2.1. Raw materials

Poly(L-lactic acid) (PLLA) (LACEA, Mitsui Chemicals Co. Ltd., Japan) and two kinds of poly(D,L-lactide-*co*-glycolide) (PDLLG) (Purasorb®; lactide:glycolide = 75:25 and 50:50; Corbion Purac Biomaterials, The Netherlands) were used in this work. According to the ratio of lactide to glycolide in PDLLG (75:25 and 50:50), they were named as PDLLG75 and PDLLG50, respectively. The molecular weights of PLLA, PDLLG75, and PDLLG50 were 140, 170, and 170 kDa, respectively.

MgSiV particles were prepared using a carbonation method described in our previous report [17]. Briefly, 133.4 g of $Ca(OH)_2$ was dissolved in a co-solvent containing 2000 mL of methanol and 200 mL of distilled water (DW). After CO_2 gas was blown in the solution for 20 min, 11.7 g of $Mg(OH)_2$ and 60 mL of 3-aminopropyltriethoxysilane (APTES) were added into the slurry, which was stirred for another 40 min while CO_2 was being blown. The resulting slurry was dried at 110 °C to obtain MgSiV particles (diameter ~1 μm). The silicon and magnesium contents of the MgSiV particles were estimated to be 2.8 and 2.0 mass% by inductively coupled plasma atomic emission spectroscopy (ICP-AES).

2.2. Preparation of MgSiV-polymer composite films

To prepare the MgSiV-polymer composites, MgSiV particles were initially kneaded with the polymers. The ratio of polymer to MgSiV was 53:47 (vol%) (40:60 in mass%). 28 g of the polymer was poured into a pre-heated kneading reactor and held for 5 min for melting and then 42 g of the MgSiV particles was added into the reactor and kneading was carried out for 15 min. The processing temperatures were set at 190 °C for PLLA, 130 °C for PDLLG75, and 110 °C for PDLLG50.

A solution-casting method was employed to prepare the composite films. Four grams of the kneaded composites were dissolved in 40 g of chloroform and stirred in a capped vessel for 6 h at room temperature. The MgSiV-polymer composite solution was poured into a glass culture dish (ø = 90 mm) to evaporate the solvent. After the cast solutions were dried for 1 d, composite films with ~0.3 mm thickness were obtained. The resulting composite films are denoted as MgSiV-PLLA, MgSiV-PDLLG75, and MgSiV-PDLLG50.

2.3. Surface morphologies

The surface and fracture morphologies of the composite films were observed using a scanning electron microscope (SEM, JSM-6301F, JEOL, Japan) after the specimens were coated with a thin layer of platinum. The cross-sections, obtained by breaking the films soaked in liquid nitrogen for 2 min with tweezers, were observed to analyze the fracture face morphologies. To characterize the crystalline phases, X-ray diffraction (XRD, X'pert X-ray diffractometer,

Philips; Cu*K*α, 50 kV, 40 mA) was carried out. The scanning rate was 1°/min.

2.4. Ion release behavior

The ion releasing behavior of the composite films was evaluated in TBS as described previously [17]. The preparation of TBS was carried out as follows – initially, 6.118 g of tris(hydroxymethyl) aminomethane was dissolved in 1000 mL DW at 37 °C and the pH of the solution was adjusted to 7.4 with 1 M hydrochloric acid. To examine the dissolution behavior of the composite films, each film of ~0.3 mm thickness was cut into square-shaped samples (20 mm×20 mm), which were soaked in 10 mL TBS in a polystyrene vessel. The vessel was sealed and stored statically in an incubator at 37 °C. At predetermined time intervals (1 h~7 d), the soaked samples were taken out from the solution, rinsed with DW, and dried at room temperature; meanwhile, the Mg^{2+}, Ca^{2+}, and silicate ions contents in the solutions were analyzed. The experiments were performed in triplicate at each time point for statistical relevance.

The concentrations of the Mg^{2+}, Ca^{2+}, and silicate ions in the solutions after soaking the samples were measured by ICP-AES (ICPS-500, Shimadzu, Japan). Calibration curves were generated using magnesium, calcium, and silicon standard solutions at 1, 10, and 50 $mg \cdot mL^{-1}$. The pH values of the solutions were measured using a potentiometric pH meter (F-73T, HORIBA Ltd., Japan) at room temperature.

3. Results and discussion

3.1. Surface morphology

Figure 1 shows the SEM images of the composite films before and after being soaked in TBS. Before the samples were soaked, MgSiV particles were found to be spread on the film surfaces homogeneously.

Immediately after soaking the films in TBS, MgSiV particles on the film surface started to dissolve. After 1 h, the amount of particles decreased and numerous pores, which were comparable in size with the particles (~1 μm), were observed on the surfaces. These phenomena are thought to originate from the rapid dissolution of MgSiV particles on the surface of the composite films, which were covered with a thin polymer layer that would dissolve within 1 h; during soaking, the thin polymer layers were rapidly hydrolyzed and degraded and the particles could dissolve in the solution.

After 1 d, new needle-like products precipitated on the surface of the samples. In the case of MgSiV-PLLA, there were almost no changes in the sizes and number of surface pores while the number of needle-like products increased. In the case of PDLLG-based composites, after day 3, the number of ~1 μm sized pores decreased and larger pores appeared, which implies the degradation of PDLLG matrices. After day 3, numerous cube-like products were observed on MgSiV-PDLLG50.

Figure 2 shows the XRD patterns of the composite films before and after soaking them in TBS. The patterns clearly show the phase transformation of calcium carbonate crystals. Before soaking, the composites were characterized by the strong diffraction peaks originating from vaterite phase in the MgSiV particles, containing a small amount of calcite [23]. After 1 d of soaking, the peak intensities of vaterite in all the samples reduced and peaks corresponding to aragonite appeared. The new needle-like products are believed to be aragonite crystals. After 7 d of soaking, strong peaks corresponding to aragonite were observed in the diffractograms of MgSiV-PLLA and MgSiV-PDLLG75. It has been reported that aragonite is formed in a carbonation process when the aqueous solution contains Mg^{2+} ions [24–27]. The existence of Mg^{2+} ions in the solution modifies the nucleation kinetics in the crystallization process of calcium carbonates. The growth rate of calcite decreases while that of aragonite is unaffected [26, 27]. In the case of MgSiV-PDLLG50, after 7 d of soaking, strong diffraction peaks corresponding to calcite were observed. The cube-like products are believed to be calcite crystals. The XRD patterns and the surface morphologies (Figure 1) suggest that, at day 7, calcite was the dominant crystal phase in MgSiV-PDLLG50.

3.2. Ion release behavior

Figure 3 shows the cumulative amounts of Mg^{2+}, Ca^{2+}, and silicate ions released from the composite films after they were soaked in TBS. Silicate ion release was measured in terms of silicon ion release from a calibration curve generated using the standard solution for ICP-AES.

The amount of Mg^{2+} ions released from the PDLLG-based composite films increased rapidly within 3 d, after which the release was almost constant due to discontinuous release. In other words, almost all of the Mg^{2+} ions embedded in the PDLLG-based samples

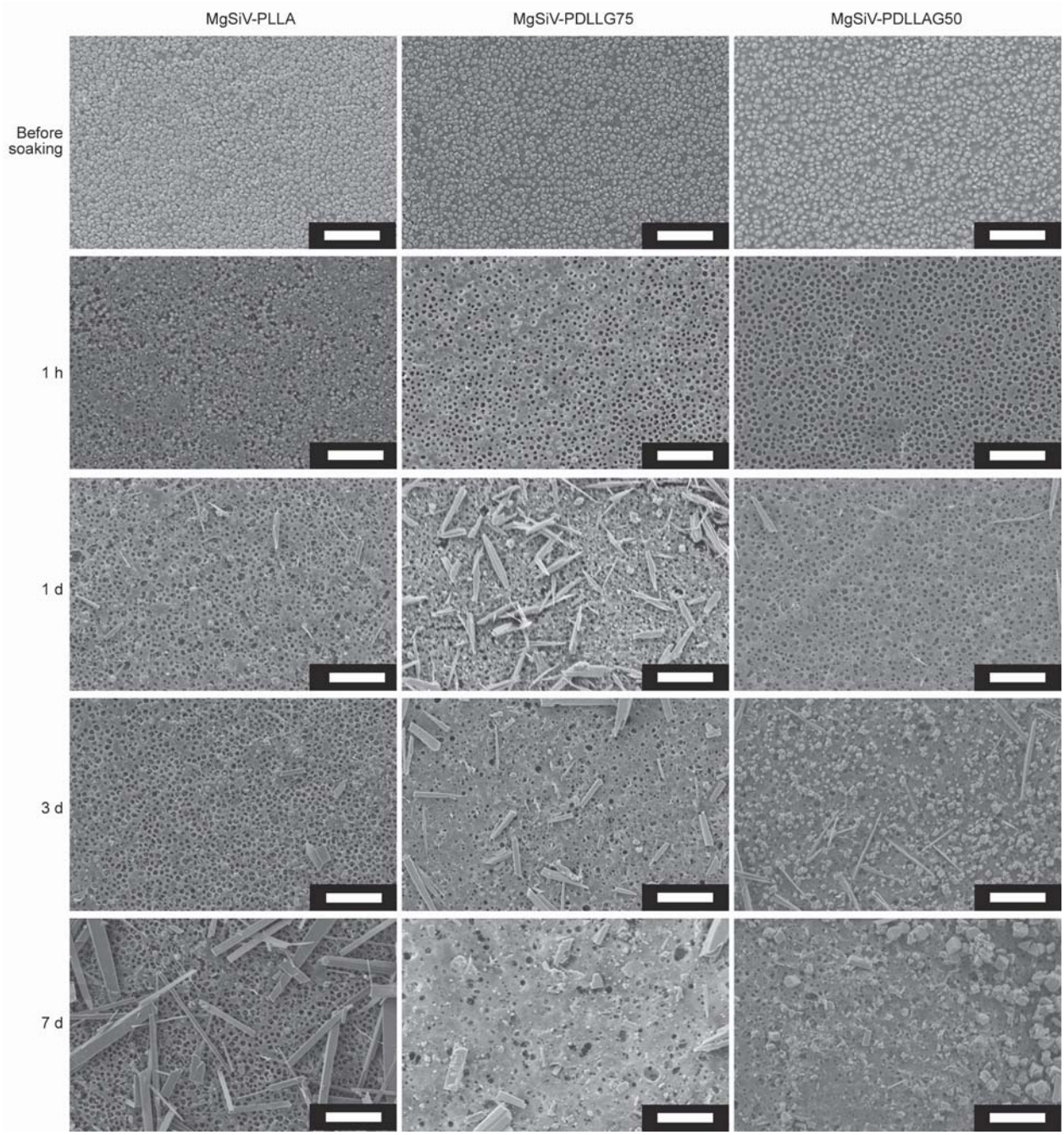

Figure 1. SEM images of the composite films before and after soaking in TBS for 1 h~7 d. The scale bar is 10 μm.

were dissolved within 3 d of soaking in TBS. On the other hand, in the case of Mg^{2+} ion release from MgSiV-PLLA, the cumulative release amounts were always smaller than those of the PDLLG-based samples; furthermore, a continuous increase in the amount of the released Mg^{2+} ions was observed. After 7 d of soaking, ~70% of the magnesium in the intact sample was estimated to have been released. The Mg^{2+} ion release behavior might originate from the chemical structure of MgSiV. During processing, Mg^{2+} ions form Mg–O–Si bonds and aggregate on the surface of calcium carbonate through a deprotonated OH group bonding with Ca^{2+} ions [17, 28]. Ca^{2+} ions were released rapidly from MgSiV-PLLA and MgSiV-PDLLG75 within 12 h (~10% of calcium content in the original samples); after day 1, the released Ca^{2+} ion content decreased and was almost constant until 7 d. In the case of MgSiV-PDLLG50, Ca^{2+} ions were released rapidly within 12 h, and the released contents were high at day 3 and day 7. The silicate ion release behavior was similar to that of Mg^{2+} ion. Within 3 d, almost all of the silicate ions were released (80~100% of silicon content in the original samples). In the case of MgSiV-PLLA, the

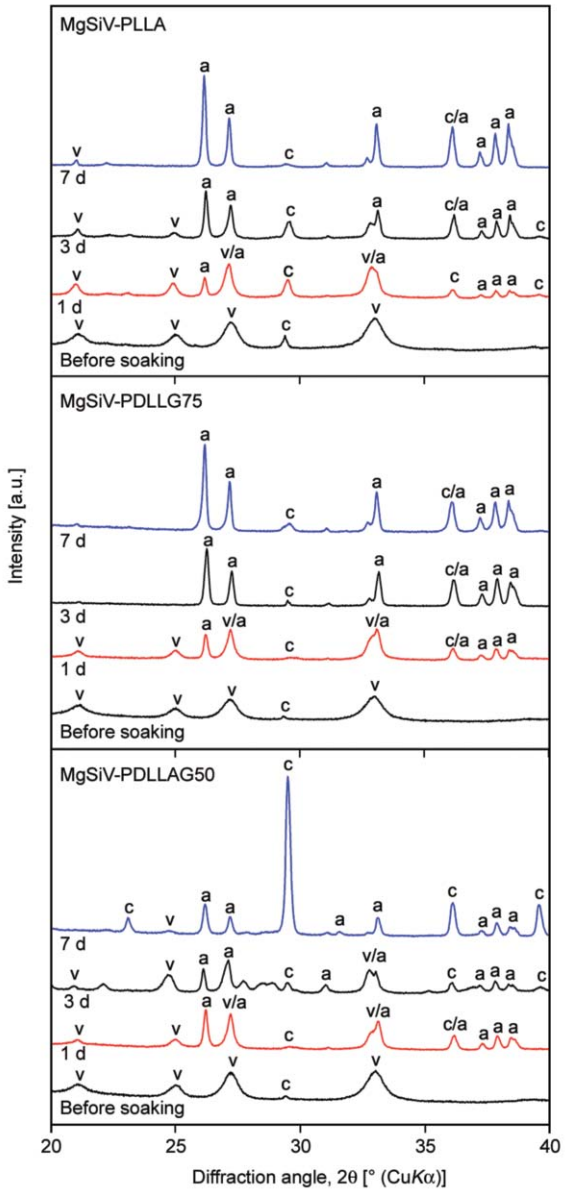

Figure 2. XRD patterns of the composite films before and after soaking in TBS for 7 days. a = aragonite, v = vaterite, and c = calcite.

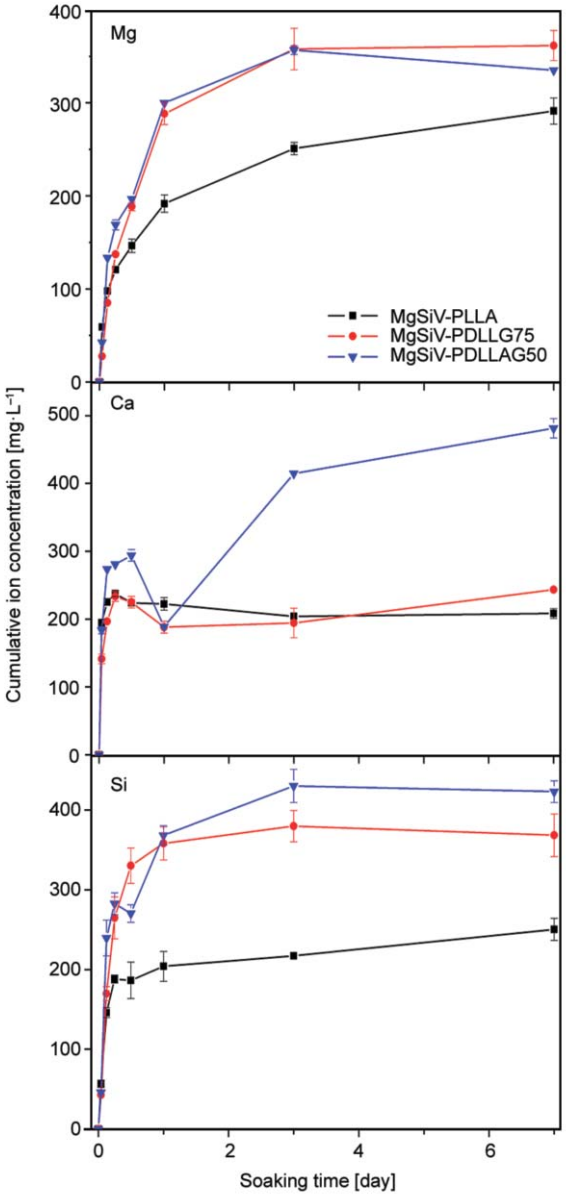

Figure 3. Mg^{2+}, Ca^{2+}, and silicate ion release profiles after soaking the composite films in TBS at 37 °C. The error bars indicate standard deviation.

release of silicate ions was suppressed relatively after 12 h.

The rapid release of the silicate ions within 12 h is considered to be due to the dissolution of the MgSiV particles on the surfaces of the films. Immediately after the films were exposed to TBS, dissolution started. For example, consider the case of MgSiV-PDLLG75. As shown in Figure 4, at hour 1, a homogeneous distribution of the MgSiV particles could be seen on the surface; pores were formed when these particles dissolved. The composites include ~50 vol% MgSiV particles, which are embedded in the polymer matrix phase and some of the particles might be in contact with other particles. When the particles dissolved, pores were left in the matrix and continuous pores, if any, transformed into channels. In our previous work [29], when PDLLG75 was coated on a material with Ca^{2+} and silicate ion release capability, the resulting material's release kinetics followed the Weibull model, showing a purely diffusive release after the hydration of the PDLLG75 layer. In this work, because of the water uptake ability of PDLLGs, the MgSiV particles embedded tightly in the polymer matrix dissolve and ions diffuse through both the channel and the PDLLG matrix. After day 3, almost no MgSiV particles could be observed and some new products formed inside the porous samples. In the case of PDLLA-based composites, it is

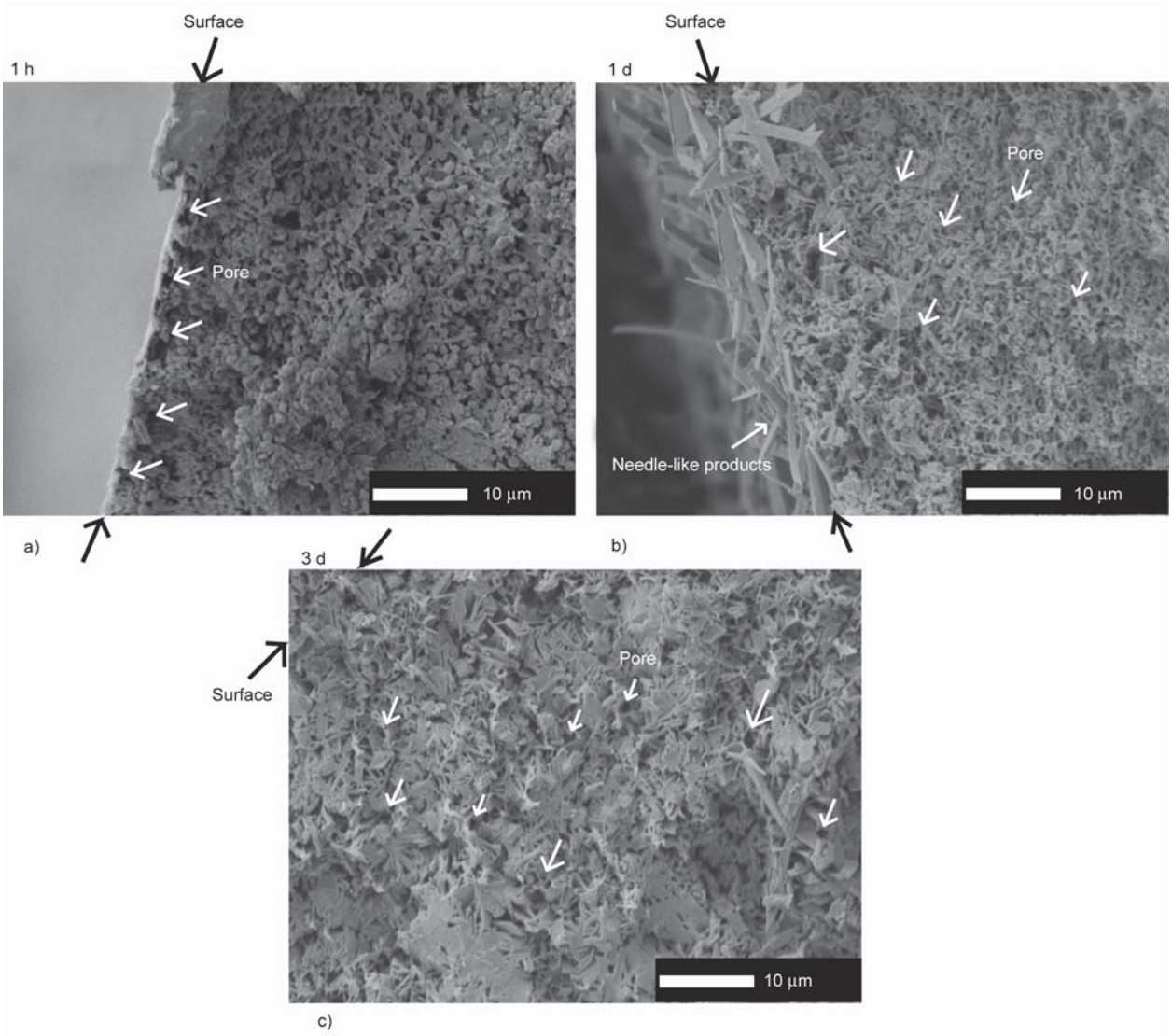

Figure 4. Cross-sectional SEM images of MgSiV-PDLLG75 fracture samples after films were soaked in TBS for a) 1 h, b) 1 d, and c) 3 d.

believed that the absorption-diffusion model comes into play immediately after the films are soaked in TBS.

In Figure 3, slight decreases in the cumulative amounts of Mg^{2+} and silicate ions were observed. Although this might be in the region of measurement error, the possibility of adsorption to form new products around the sample surface might be also considered. Experiment for clarifying this phenomenon is in progress.

The amount of ions released from MgSiV-PLLA was smaller than that from PDLLG-based samples. This would be due to the strong hydrophobicity and low degradability of PLLA. The extra methyl group in the PLLA repeating unit reduces its molecular affinity to water and leads to slow hydrolysis [30]. Therefore, the penetration of TBS into the composite is very slow and it takes a long time for the particles embedded in the PLLA matrix to be exposed to TBS. As a result, the release of ions is controlled. The routes for ions release from MgSiV-PLLA are believed to be developed by the dissolution of MgSiV particles on the surface and agglomerated ones; thus, the absorption-diffusion model cannot suitably explain the release behavior in this case.

Figure 5 shows the pH values of TBS after soaking the samples. In the case of MgSiV-PLLA and MgSiV-PDLLG75, the values increased until day 3. Mg^{2+}, Ca^{2+}, and silicate ions released from the MgSiV particles on the surface would increase the pH value of TBS. As a result, the degradation of PLLA and PDLLG75 might be promoted slightly [20]. As the released ion content reduced after 3~7 d, the pH values were almost constant. In Figure 3, the cumulative

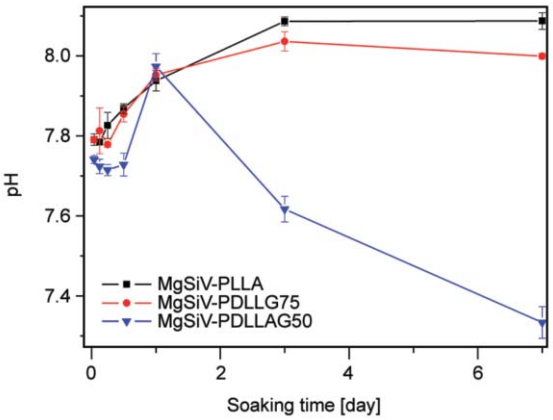

Figure 5. The pH values of TBS (at 37 °C) after soaking the composite films. The error bars indicate standard deviation.

amounts of Ca^{2+} ions released from the composites were found to increase up to 12 h of soaking, after which they decreased to ~200 mg·L^{-1}, which then remained constantly. After 1 d, the formation of aragonite took place (Figures 1 and 2). Aragonite has been reported to form in Mg^{2+} ion-containing aqueous solutions at pH > ~8 with needle-like shapes [24]. In other words, Ca^{2+} ions released from MgSiV were consumed to form aragonite crystals.

On the other hand, the solution in which MgSiV-PDLLG50 was soaked, exhibited different Ca^{2+} ion content and pH values (in Figures 3 and 5, respectively). PDLLG50 has been reported to have the highest degradability among the various PDLLG systems available [22]. The decrease in the pH of the solution is considered to be due to the rapid hydrolysis of the polymer chains [20]. As a result, the release of Ca^{2+} ions is accompanied by a decrease in the pH. After 7 d of soaking, the pH of the solution was around 7.5 (<8). During the precipitation of calcium carbonate polymorphs, solutions with high Mg/Ca ratios tend to precipitate aragonite while those with low ratios tend to form calcite [27]. In the case of MgSiV-PDLLG50, after 1 d, the low pH would enhance the release of Ca^{2+}. As a result, the Mg/Ca ratio in the solution decreased, thus favoring calcite formation.

As described earlier, the rate of ion release from MgSiV-PLLA was slower as compared to PDLLG-based composites due to the poor water uptake ability and slow degradation rate of the PLLA matrix. Therefore, to rapidly release Mg^{2+} ions and enhance cell adhesion, PDLLG-based composites would be preferable.

However, when MgSiV-PDLLG50 is used in the body, the fast degradation of PDLLG50 would lead to a dramatic decrease in the pH of the environment around the material. The high water uptake and swelling ability of PDLLG50 could lead to wide channels and pathways, which can enhance the interaction of the particles with aqueous solutions and facilitate ion diffusion. It should also be kept in mind that the large variations in pH and amount of ions released might limit the application of these materials in bone repair.

In contrast, MgSiV-PDLLG75 is expected to exhibit a suitable ion release behavior. A large portion of the Mg^{2+} ions was dissolved out within 3 d. Ca^{2+} ions were released continuously and consumed in aragonite formation. This behavior is expected to have a beneficial effect on cell adhesion. After 3 d, the silicate ion release was almost controlled. Obata *et al*. [31] reported that when an appropriate amount of silicate ions was supplied only at the initial stages of cell culture, mineralization could be enhanced. Such phenomena are caused by the formation of pathways for ion release, originating from the water uptake ability of the polymer. As shown in Figure 1, MgSiV-PDLLG75 exhibited a healing effect on the small-sized pores on its surface after 1 d. Since the pH values after soaking MgSiV-PDLLG75 in TBS increased moderately to 7.8-8.1, no negative effect on bone-forming ability would be given.

For effectively stimulating cell activation for bone repair, the material used should exhibit desirable ion release and degradation characteristics. In this context, MgSiV-PDLLG75 is expected to be a promising candidate for bone repair. Advanced applications to medical devices with drug delivery systems using MgSiV-PDLLG75 would be also expected. The devices might be derived via various techniques, such as protein-entrapping [32], electrospinning [33], sol-gel processing [34], hydrogelation [35] and oil-spill treatment [36].

4. Conclusions

Three kinds of composites containing MgSiV particles were prepared using PLLA, PDLLG75, and PDLLG50 as the polymeric matrices. The release of Mg^{2+}, Ca^{2+}, and silicate ions from these composites in TBS was investigated. The strong hydrophobicity of PLLA controlled the release of ions from the MgSiV-PLLA composite. The fast degradation of

PDLLG50 induced a decrease in the pH of the TBS soaking solution. During a 7 d period, MgSiV-PDLLG75 composites exhibited continuous ion release and the pH of the soaking solution was found to be steady; these composites exhibited desirable water uptake ability and degradability, which helped in the creation of pathways for ion release and diffusion. Therefore, it is concluded that MgSiV in combination with PDLLG75 is suitable for use in bone repair applications.

Acknowledgements

The present work was conducted in the framework of the Academic Unit Cooperation Program between Nagoya Institute of Technology (NITech) and Imperial College, London (ICL). The authors are indebted to Dr. Anthony L. B. Maçon (NITech and ICL) for his valuable input. The present work was supported in part by the JSPS Program for Advancing Strategic International Networks to Accelerate the Circulation of Talented Researchers.

References

[1] Ma P. X.: Scaffolds for tissue fabrication. Materials Today, **7**, 30–40 (2004). https://doi.org/10.1016/S1369-7021(04)00233-0

[2] Amini A. R., Laurencin C. T., Nukavarapu S. P.: Bone tissue engineering: Recent advances and challenges. Critical Reviews™ in Biomedical Engineering, **40**, 363–408 (2012). https://doi.org/10.1615/CritRevBiomedEng.v40.i5.10

[3] Bose S., Tarafder S.: Calcium phosphate ceramic systems in growth factor and drug delivery for bone tissue engineering: A review. Acta Biomaterialia, **8**, 1401–1421 (2012). https://doi.org/10.1016/j.actbio.2011.11.017

[4] Gentile P., Chiono V., Carmagnola I., Hatton P. V.: An overview of poly(lactic-*co*-glycolic) acid (PLGA)-based biomaterials for bone tissue engineering. International Journal of Molecular Sciences, **15**, 3640–3659 (2014). https://doi.org/10.3390/ijms15033640

[5] Vergnol G., Ginsac N., Rivory P., Meille S., Chenal J-M., Balvay S., Chevalier J., Hartmann D. J.: *in vitro* and *in vivo* evaluation of a polylactic acid-bioactive glass composite for bone fixation devices. Journal of Biomedical Materials Research Part B: Applied Biomaterials, **104**, 180–191 (2016). https://doi.org/10.1002/jbm.b.33364

[6] Verrier S., Blaker J. J., Maquet V., Hench L. L., Boccaccini A. R.: PDLLA/Bioglass® composites for soft-tissue and hard-tissue engineering: An *in vitro* cell biology assessment. Biomaterials, **25**, 3013–3021 (2004). https://doi.org/10.1016/j.biomaterials.2003.09.081

[7] Tsigkou O., Hench L. L., Boccaccini A. R., Polak J. M., Stevens M. M.: Enhanced differentiation and mineralization of human fetal osteoblasts on PDLLA containing Bioglass® composite films in the absence of osteogenic supplements. Journal of Biomedical Materials Research Part A, **80A**, 837–851 (2007). https://doi.org/10.1002/jbm.a.30910

[8] Tsigkou O., Jones J. R., Polak J. M., Stevens M. M.: Differentiation of fetal osteoblasts and formation of mineralized bone nodules by 45S5 Bioglass® conditioned medium in the absence of osteogenic supplements. Biomaterials, **30**, 3542–3550 (2009). https://doi.org/10.1016/j.biomaterials.2009.03.019

[9] Xynos I. D., Edgar A. J., Buttery L. D. K., Hench L. L., Polak J. M.: Gene-expression profiling of human osteoblasts following treatment with the ionic products of Bioglass® 45S5 dissolution. Journal of Biomedical Materials Research Part A, **55**, 151–157 (2001). https://doi.org/10.1002/1097-4636(200105)55:2<151::AID-JBM1001>3.0.CO;2-D

[10] Jones J. R.: Review of bioactive glass: From Hench to hybrids. Acta Biomaterialia, **9**, 4457–4486 (2013). https://doi.org/10.1016/j.actbio.2012.08.023

[11] Hoppe A., Güldal N. S., Boccaccini A. R.: A review of the biological response to ionic dissolution products from bioactive glasses and glass-ceramics. Biomaterials, **32**, 2757–2774 (2011). https://doi.org/10.1016/j.biomaterials.2011.01.004

[12] Marie P. J.: The calcium-sensing receptor in bone cells: A potential therapeutic target in osteoporosis. Bone, **46**, 571–576 (2010). https://doi.org/10.1016/j.bone.2009.07.082

[13] Maniatopoulos C., Sodek J., Melcher A. H.: Bone formation *in vitro* by stromal cells obtained from bone marrow of young adult rats. Cell and Tissue Research, **254**, 317–330 (1988). https://doi.org/10.1007/BF00225804

[14] Mastrogiacomo M., Papadimitropoulos A., Cedola A., Peyrin F., Giannoni P., Pearce S. G., Alini M., Giannini C., Guagliardi A., Cancedda R.: Engineering of bone using bone marrow stromal cells and a silicon-stabilized tricalcium phosphate bioceramic: Evidence for a coupling between bone formation and scaffold resorption. Biomaterials, **28**, 1376–1384 (2007). https://doi.org/10.1016/j.biomaterials.2006.10.001

[15] Zreiqat H., Howlett C. R., Zannettino A., Evans P., Schulze-Tanzil G., Knabe C., Shakibaei M.: Mechanisms of magnesium-stimulated adhesion of osteoblastic cells to commonly used orthopaedic implants. Journal of Biomedical Materials Research Part A, **62**, 175–184 (2002). https://doi.org/10.1002/jbm.10270

[16] Yoshizawa S., Brown A., Barchowsky A., Sfeir C.: Magnesium ion stimulation of bone marrow stromal cells enhances osteogenic activity, simulating the effect of magnesium alloy degradation. Acta Biomaterialia, **10**, 2834–2842 (2014). https://doi.org/10.1016/j.actbio.2014.02.002

[17] Yamada S., Ota Y., Nakamura J., Sakka Y., Kasuga T.: Preparation of siloxane-containing vaterite doped with magnesium. Journal of the Ceramic Society of Japan, **122**, 1010–1015 (2014). https://doi.org/10.2109/jcersj2.122.1010

[18] Yamada S., Obata A., Maeda H., Ota Y., Kasuga T.: Development of magnesium and siloxane-containing vaterite and its composite materials for bone regeneration. Frontiers in Bioengineering and Biotechnology, **3**, 195/1–195/9 (2015). https://doi.org/10.3389/fbioe.2015.00195

[19] Wu X. S.: Synthesis, characterization, biodegradation, and drug delivery application of biodegradable lactic/glycolic acid polymers: Part III. Drug delivery application. Artificial Cells, Blood Substitutes, and Biotechnology, **32**, 575–591 (2004). https://doi.org/10.1081/BIO-200039635

[20] Alexis F.: Factors affecting the degradation and drug-release mechanism of poly(lactic acid) and poly[(lactic acid)-*co*-(glycolic acid)]. Polymer International, **54**, 36–46 (2005). https://doi.org/10.1002/pi.1697

[21] Anderson J. M., Shive M. S.: Biodegradation and biocompatibility of PLA and PLGA microspheres. Advanced Drug Delivery Reviews, **64**, 72–82 (2012). https://doi.org/10.1016/j.addr.2012.09.004

[22] Carmagnola I., Nardo T., Gentile P., Tonda-Turo C., Mattu C., Cabodi S., Defilippi P., Chiono V.: Poly(lactic acid)-based blends with tailored physicochemical properties for tissue engineering applications: A case study. International Journal of Polymeric Materials and Polymeric Biomaterials, **64**, 90–98 (2015). https://doi.org/10.1080/00914037.2014.886247

[23] Kontoyannis C. G., Vagenas N. V.: Calcium carbonate phase analysis using XRD and FT-Raman spectroscopy. Analyst, **125**, 251–255 (2000). https://doi.org/10.1039/a908609i

[24] Ota Y., Inui S., Iwashita T., Kasuga T., Abe Y.: Preparation of aragonite whiskers. Journal of the American Ceramic Society, **78**, 1983–1984 (1995). https://doi.org/10.1111/j.1151-2916.1995.tb08924.x

[25] Fernandez-Diaz L., Putnis A., Prieto M., Putnis C. V.: The role of magnesium in the crystallization of calcite and aragonite in a porous medium. Journal of Sedimentary Research, **66**, 482–491 (1996). https://doi.org/10.1306/d4268388-2b26-11d7-8648000102c1865d

[26] Loste E., Wilson R. M., Seshadri R., Meldrum F. C.: The role of magnesium in stabilising amorphous calcium carbonate and controlling calcite morphologies. Journal of Crystal Growth, **254**, 206–218 (2003). https://doi.org/10.1016/S0022-0248(03)01153-9

[27] De Choudens-Sanchez V., Gonzalez L. A.: Calcite and aragonite precipitation under controlled instantaneous supersaturation: Elucidating the role of $CaCO_3$ saturation state and Mg/Ca ratio on calcium carbonate polymorphism. Journal of Sedimentary Research, **79**, 363–376 (2009). https://doi.org/10.2110/jsr.2009.043

[28] Nakamura J., Poologasundarampillai G., Jones J. R., Kasuga T.: Tracking the formation of vaterite particles containing aminopropyl-functionalized silsesquioxane and their structure for bone regenerative medicine. Journal of Materials Chemistry B, **1**, 4446–4454 (2013). https://doi.org/10.1039/c3tb20589d

[29] Zhou P., Wang J., Maçon A. L., Obata A., Jones J. R., Kasuga T.: Tailoring the delivery of therapeutic ions from bioactive scaffolds while inhibiting their apatite nucleation: A coaxial electrospinning strategy for soft tissue regeneration. RSC Advances, **7**, 3992–3999 (2017). https://doi.org/10.1039/C6RA25645G

[30] Damadzadeh B., Jabari H., Skrifvars M., Airola K., Moritz N., Vallittu P. K.: Effect of ceramic filler content on the mechanical and thermal behaviour of poly-L-lactic acid and poly-L-lactic-*co*-glycolic acid composites for medical applications. Journal of Materials Science: Materials in Medicine, **21**, 2523–2531 (2010). https://doi.org/10.1007/s10856-010-4110-9

[31] Obata A., Iwanaga N., Terada A., Jell G., Kasuga T.: Osteoblast-like cell responses to silicate ions released from 45S5-type bioactive glass and siloxane-doped vaterite. Journal of Materials Science, **52**, 8942–8956 (2017). https://doi.org/10.1007/s10853-017-1057-y

[32] Kudryavtseva V. L., Zhao L., Tverdokhlebov S. I., Sukhorukov G. B.: Fabrication of PLA/$CaCO_3$ hybrid microparticles as carriers for water-soluble bioactive molecules. Colloids and Surfaces B: Biointerfaces, **157**, 481–489 (2017). https://doi.org/10.1016/j.colsurfb.2017.06.011

[33] Mei L., Wang Y., Tong A., Guo G.: Facile electrospinning of an efficient drug delivery system. Expert Opinion on Drug Delivery, **13**, 741–753 (2016). https://doi.org/10.1517/17425247.2016.1142525

[34] Fan R., Deng X. H., Zhou L. X., Gao X., Fan M., Wang Y. L., Guo G.: Injectable thermosensitive hydrogel composite with surface-functionalized calcium phosphate as raw materials. International Journal of Nanomedicine, **9**, 615–626 (2014). https://doi.org/10.2147/IJN.S52689

[35] Yang H-Y., Niu L-N., Sun J-L., Huang X-Q., Pei D-D., Huang C., Tay F. R.: Biodegradable mesoporous delivery system for biomineralization precursors. International Journal of Nanomedicine, **12**, 839–854 (2017). https://doi.org/10.2147/IJN.S128792

[36] Kalliola S., Repo E., Srivastava V., Heiskanen J. P., Sirviö J. A., Liimatainen H., Sillanpää M.: The pH sensitive properties of carboxymethyl chitosan nanoparticles cross-linked with calcium ions. Colloids and Surfaces B: Biointerfaces, **153**, 229–236 (2017). https://doi.org/10.1016/j.colsurfb.2017.02.025